REGULAR PAPER

Large Area Organic Thin Film Coating Using a Micro Multi-nozzle Jet Head with Side Suction Channels

Kwon-Yong Shin[1] · Mingyu Kang[2] · Myong-Ki Kim[3] · Ki Sung Jung[4] · Chun Sang Yoo[4] · Kyung-Tae Kang[1] · Sang-Ho Lee[1]

Abstract

In this paper, we propose a unique micro multi-nozzle jet head to generate a stable column jet flow by applying vacuum suction to the side of a jetting nozzle. The micro multi-nozzle jet head was designed and fabricated to operate in both the jetting and suction modes selectively or simultaneously. The jet head includes eighteen jetting nozzles of 100 µm diameter, vacuum suction channels, inlets and a nozzle protection outer hole. The whole size of the micro multi-nozzle jet plate is 50×20 mm^2. To demonstrate large area organic thin film coating, micro multi-nozzle jet coating was performed on a 5th generation size (1100×1300 mm^2) glass substrate. A poly(3,4-ethylenedioxythiophene):poly(styrene sulfonate) (PEDOT:PSS) solution was selected as a test ink. To uniformly coat an organic thin film, we first investigated the physical parameter conditions such as jetting pressure, head suction pressure, stage moving speed, and coating head printing pitch. The thickness of the coated PEDOT:PSS thin film was 76.86 ± 3.33 nm and its uniformity (CV) was 4.33%.

Keywords Large area · Coating · Organic thin film · Multi-nozzle jet · Suction channels

1 Introduction

Optoelectronic devices based on organic semiconductors, including conjugated small molecules and polymers, have attracted tremendous attention from both academic and industrial circles, due to the many technological advantages of organic materials, such as low material cost, outstanding diversity, tunable material properties, compatibility with flexible substrates, and low temperature/high throughput manufacturing processes [1–4].

The most advanced organic electronic systems already in commercial production are high efficiency, very bright, and colorful thin displays based on OLEDs. As a flat-panel light source, OLED shave drawn huge attention due to their superior features such as large area surface emission, flexibility, transparency, etc. [5–7]. A vacuum thermal evaporation method is currently considered a suitable process for

✉ Sang-Ho Lee
  sholee7@kitech.re.kr

  Kwon-Yong Shin
  sky@kitech.re.kr

  Mingyu Kang
  whitymk@snu.ac.kr

  Myong-Ki Kim
  mk-kim@deviceeng.co.kr

  Ki Sung Jung
  kisung8.jung@unist.ac.kr

  Chun Sang Yoo
  csyoo@unist.ac.kr

  Kyung-Tae Kang
  ktkang@kitech.re.kr

[1] Korea Institute of Industrial Technology, 143 Hanggaul-ro, Sangnok-gu, Ansan-si, Gyeonggi-do 15588, Republic of Korea

[2] Program in Nanoscience and Technology, Graduate School of Convergence Science and Technology, Seoul National University, Seoul 08826, Republic of Korea

[3] DEVICEENG Co., LTD., 169, Eumbong-myeon, Asan-si, Chungcheongnam-do 336-864, Republic of Korea

[4] Department of Mechanical Engineering, Ulsan National Institute of Science and Technology (UNIST), UNIST-Gil 50, Ulsan 44919, Republic of Korea

realizing multi-layer architectures, which are required for highly efficient and long life OLEDs. However, the vacuum thermal evaporation based process faces disadvantages in terms of fabrication and investment costs. High manufacturing costs are one of the factors that make it difficult to successfully enter the various application markets despite the many advantages of OLEDs. Solution-process techniques are highly demanded to reduce fabrication costs in OLEDs [7, 8]. Several wet film deposition techniques have been investigated for solution processing of OLEDs in the past. The deposition techniques can be categorized into printing technologies (inkjet printing, gravure printing, flexo-printing, screen printing, rotary screen printing) and coating techniques (spin coating, dip coating, knife coating, spray coating, slide coating, and slot die coating) [5, 9–17]. The key issue of the wet film deposition is to obtain very uniform layers with defined interfaces to produce efficient devices. Slot-die coating has been preferred as a commercial solution-coating technique for preparing large area and uniform organic films, and this technique has been scaled up to at least Gen. 8 substrates for flat-panel-display processing. Slot-die coating is also being developed for use in general OLED lighting fabrication [18, 19]. The slot-die coating provides large scale roll-to-roll production and the simultaneous coating of multiple layers of different solutions for a wide range of process materials and depositing organic thin films having thickness as low as 20 nm [5–7, 20].

Recently, Dainippon Screen (DNS) and DuPont Displays Inc. (DDI) have introduced continuous multi-nozzle printing as an OLED patterning technology. Continuous nozzle printing utilizes a column liquid jet that issues from a fixed orifice and then impinges on the substrate. The printing process operates by continuously moving the liquid jet across the substrate in alignment with previously defined wetting and non-wetting areas. The print head traverses back and forth along the x-axis of the printed plate while the stage (substrate) proceeds in increments along the y-axis in synchronization with the head. Commercially acceptable cycle times can be obtained by printing multiple arrays of jets using x-axis traverse speeds up to 5 m/s [18, 21]. Continuous nozzle printing offers many benefits as a solution-based manufacturing system such as high throughput and scalable printing performance, a simple passive jetting mechanism, wide selectivity of printing materials, simple head fabrication process, etc.

In the case of the slot-die coating system, each time the substrate size is changed, there is a disadvantage that a heavy slot-die head of hundreds of kg must be fabricated by ultra-high precision metal processing to fit the width of the substrate. Repetitive fabrication of the heavy slot-die head to fit the substrate size is not easy to realize scalable coating required for large area organic thin film coating. The multi-nozzle printing is very useful for performing scalable coating of the organic thin film over a large area with the same multi-nozzle head due to its advantages such as high throughput and scalable printing performance [22–27]. Other previous studies on the multi nozzle printing reported a method of printing stripe patterns inside bank structure to fabricate the pixels of organic light emitting diode (OLED) display.

The research objective of this study is to develop the large area organic thin film coating method by scalable multi-nozzle jet coating. Prior to continuous nozzle printing process, it is very important to make a stable column jet flow because we can control the coating thickness by regulating the flow rate. In this study, we proposed a unique nozzle jetting method that applies vacuum suction to the side of the jetting nozzle for stable formation of a stable column jet flow. The vacuum suction was very effective in eliminating dangling droplet formation at a nozzle end, which interfere with the immediate and stable column jet flow. To realize the proposed nozzle jetting method, we fabricated the micro multi-nozzle jet head with three dimensional micro channel networks by micro fabrication process. The developed micro multi-nozzle jet head includes eighteen jetting nozzles of 100 μm diameter, suction channels, and inlet hole. A poly(3,4-ethylenedioxythiophene):poly(styrene sulfonate) (PEDOT:PSS) solution was selected as a test ink to perform the feasibility test for large area thin film coating application. To uniformly coat an organic thin film, we first investigated the physical parameter conditions such as jetting pressure, head suction pressure, stage moving speed, and coating head printing pitch.
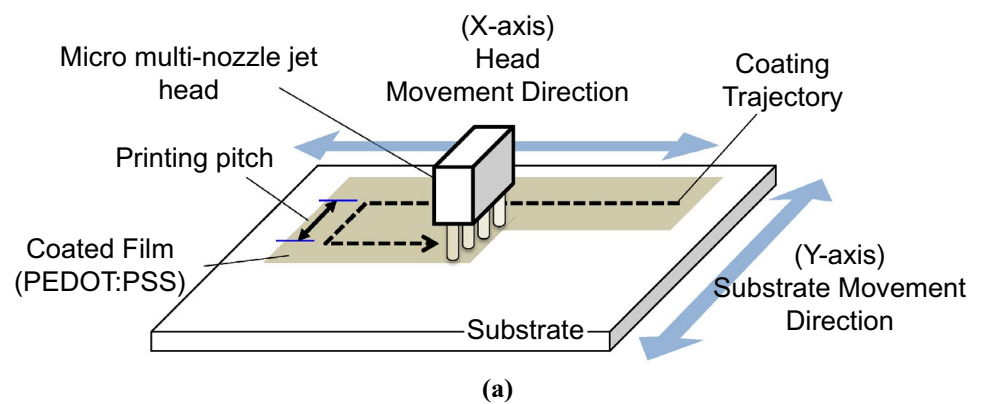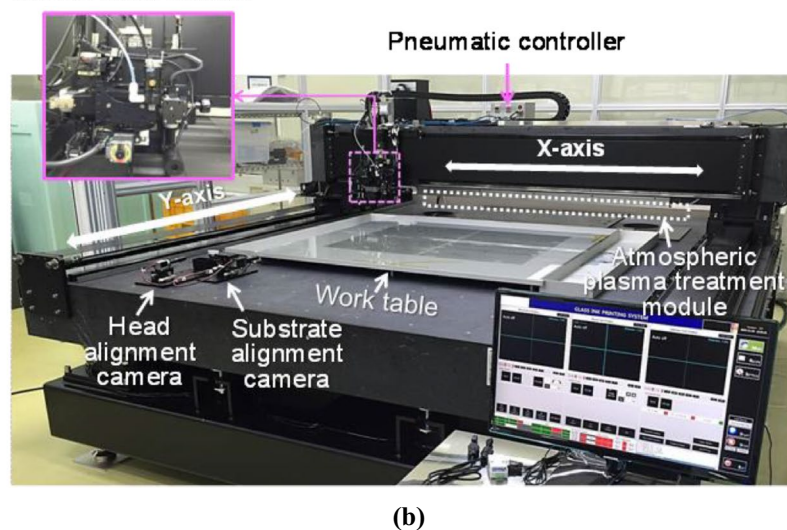
2 Experimental

2.1 Coating Methods

We used a poly(3,4-ethylenedioxythiophene):poly(styrene sulfonate) (PEDOT:PSS), (Clevios CH8000, Heraeus, Germany) aqueous solution with a concentration of 2.8 wt% to demonstrate large area and uniform coating by a micro multi-nozzle jet coating method. In this study, we prepared ink samples of pristine PEDOT:PSS diluted by ethanol 90 vol% to investigate the concentration for uniform coating of PEDOT:PSS on a substrate. PEDOT:PSS was filtered through a 0.45 μm syringe filter. Micro multi-nozzle jet coating was performed with a Gen. 5 streamjet coater (DEVICEENG, Korea) over a coating area of 1500×850 mm^2, equipped with an alignment system for substrate and nozzle alignment, a 2-channel pneumatic control ink supply system (up to 500 kPa), and an atmospheric DC plasma surface treatment system (SYSTEMKOREA, Korea) with treatment area of 1300×1600 mm^2 under ambient air. An indium tin oxide (ITO)-coated glass substrate of 1100×1300 mm^2

size was used as the substrate and its surface was treated by atmospheric plasma before starting the coating process. Operation conditions of the atmospheric plasma system are 2 kW of radio frequency power (15 ~ 40 kHz), a gap distance of 1 mm between the substrate and atmospheric plasma surface treatment system, and a moving speed of 40 mm/s. EtOH-diluted PEDOT:PSS solution was jetted through the multi-nozzle under conditions of jetting pitch of 25 ~ 40 mm, a head moving speed of 1 m/s, a coating gap distance between the nozzle and substrate of ~ 1 mm, a head suction pressure of 90 kPa, and a jetting pneumatic pressure of 180 kPa, respectively. All coating experiments were performed at 24 °C ($\pm$ 1.0 °C) and 50% ($\pm$ 5%) relative humidity. Figure 1 shows a schematic image of the large area coating method using a micro multi-nozzle jet head (Fig. 1a) and a multi-nozzle jet coating system (Fig. 1b). The micro multi-nozzle jet head traverses back and forth along the x-axis while the stage increments along the y-axis in synchronization with the head.

2.2 Nozzle Fabrication

Figure 2 shows the process flow diagram for the micro fabrication of the micro multi-nozzle jet head. First, the back side of silicon (Si) for the inlet hole is etched with ~ 200 µm depth by a Si deep RIE system (Rapier, SPTS, UK) after patterning ~ 5 µm thick photoresist (AZ4620, Allresist, Germany) as an etch mask by a photolithography process (Fig. 2a). After removal of the thick PR, 1 µm-thick SiO_2 is deposited on the top of Si substrate using a PECVD (plasma enhanced chemical vapor deposition) system (NEXSO 7000 HDPECVD, NEXSO, Korea). A SiO_2 layer is etched in a toroidal shape by a RIE system to define the micro-nozzle (RIE 80 plus, Oxford Instruments, UK) after patterning of a photoresist (PR) (AZ 5214E, MicroChemicals, Germany) (Fig. 2b). Then, a ~ 5 µm-thick PR (AZ4620, Allresist, Germany) was patterned as an etch mask and a 150 µm-deep nozzle hole was formed by a Si deep RIE system (Rapier, SPTS, UK) (Fig. 2c). After removal of the PR, Si deep RIE was carried

Fig. 1 a Schematic image of large area coating method using a micro multi-nozzle jet head, b multi-nozzle jet coating system (Gen. 5 streamjet coater, DEVI-CEENG, Korea)


(a)

(b)

Fig. 2 The process flow diagram for the micro fabrication of the micro multi-nozzle jet head: **a** silicon (Si) reactive ion etching (RIE) of the backside, **b** SiO$_2$ layer deposition and patterning, **c** Si RIE for nozzle formation on the front side, **d** photoresist (PR) removal, **e** Si RIE for through hole formation, **f** anodic bonding of the glass onto the Si structure after glass sand blasting, **g** fluorocarbon (FC) film coating on the nozzle surface
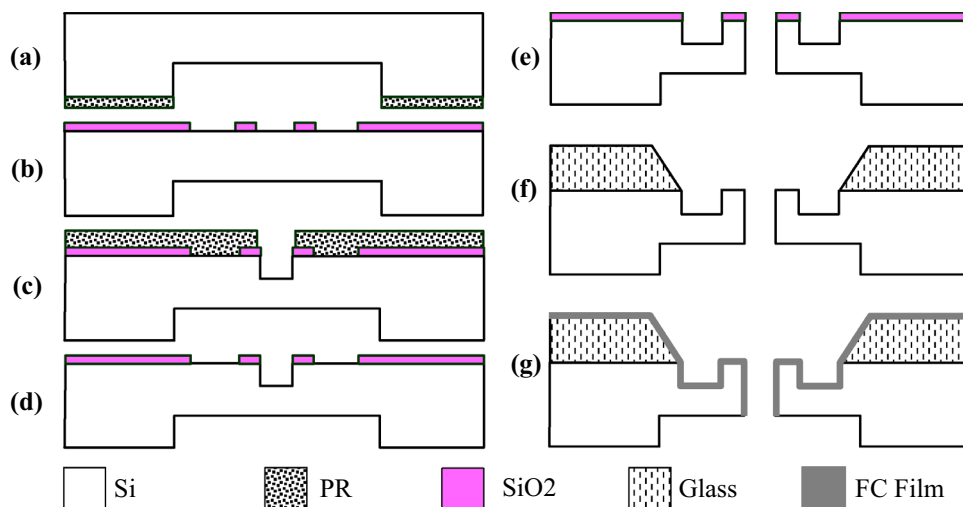
out again to form the through nozzle hole (Fig. 2d, e). The SiO$_2$ layer was removed by a buffered oxide etchant. A glass substrate was etched by sand blasting with a dry film resist etch mask (MS7100, Mitsubishi Paper Mills, Japan) to form a circular opening that matched the micro nozzles. Finally, the glass substrate with the circular opening was aligned and bonded by an anodic bonding system (SB6, SUSS MicroTec, Germany) onto the silicon substrate with the micro nozzle structure (Fig. 2f). Finally, a hydrophobic fluorocarbon (FC) film was coated on the top surface of the fabricated micro multi-nozzle to prevent spreading of the ink solution on the nozzle surface during jetting (Fig. 2g). The FC coating process was carried out by a polymer deposition process in a Si deep RIE system (Rapier, SPTS, UK).

2.3 Measurement

The film thickness of the coated PEDOT:PSS films on the substrate was measured using a spectral reflectance system (F30, Filmetrics Inc.). An Atomic Force Microscope (AFM) (NX 10, Park Systems Corp.) was used to measure the film surface roughness uniformity, and SEM was used for analysis of the cross-sectional structure of the fabricated micro multi-nozzle and coated PEDOT:PSS film.

3 Results and Discussion

Prior to development of the micro multi-nozzle jet head, we tested the effects of the number of nozzles on the uniformity of flow rate of each nozzle by simulating the flow patterns with different numbers of nozzles using a commercial software (COMSOL Multiphysics® v. 5.4., COMSOL AB, Stockholm, Sweden). Figure 3 shows a schematic of a micro multi-nozzle jet head (Fig. 3a), and 3-D computational fluid dynamics (CFD) simulation results (Fig. 3b–d):

velocity magnitude isoconours and velocity vectors for two-, three-, and four-nozzle jets with different nozzle diameter ($\phi = 0.05 \sim 2$ mm) and different distance between two neighboring nozzles ($L = 1 \sim 3$ mm). To quantitatively identify the uniformity of flow rate of each nozzle, we measure the flow rate ratio at two different nozzles, Q_1/Q_2, as a function of the nozzle diameter for three- and four-nozzle jets. Note that since the flow pattern is symmetric for the two-nozzle jet, we do not include its result in the Fig. As readily observed from Fig. 4, for the three-nozzle jet the volume flow rate at the center nozzle is slightly higher than that at the side nozzle, while the difference in the volume flow rates between the two nozzles nearly disappears when the nozzle diameter becomes large enough (e.g., $Q_1/Q_2 \approx 0.99$ at 200 μm). For the four-nozzle jet, however, the volume flow rates at the two different nozzles are nearly identical regardless of the nozzle diameter such that Q_1/Q_2 is found to be unity. Note that the effect of the distance between two neighboring nozzles on Q_1/Q_2 is found to be negligible. From the simulation results, it can be deduced that we could obtain nearly-identical volume flow rates at different nozzles of 100 μm nozzle diameter when even number of nozzles is utilized.

The micro multi-nozzle jet head was successfully fabricated by the proposed micro fabrication process as shown in Fig. 5a. Eighteen nozzles of 100 μm diameter were formed with 2 mm interval and the nozzles were divided into two, and two suction channels were connected to the upper side of the nozzle. The whole size of the micro multi-nozzle jet plate is 50×20 mm^2. Figure 5b is a microscopic image of Si microstructure with a jetting nozzle and a suction channel before the glass bonding process. Figure 5c is a microscopic image of the microstructure of the completed micro nozzle jet plate with an outer hole upward of the Si micro structure after the glass bonding process. We formed the key structures including a jetting nozzle, suction channels and inlets on the Si substrate, and an outer hole on the glass substrate
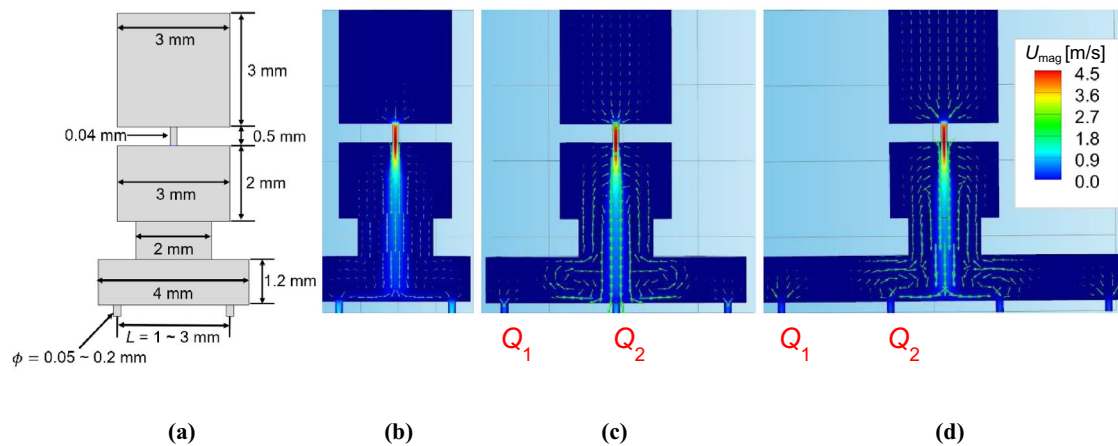
Fig. 3 **a** Schematic of a micro multi-nozzle jet head and 3-D CFD simulation results: velocity magnitude isocontours (m/s) and velocity vectors (arrows) for **b** two-, **c** three-, and **d** four-nozzle jets
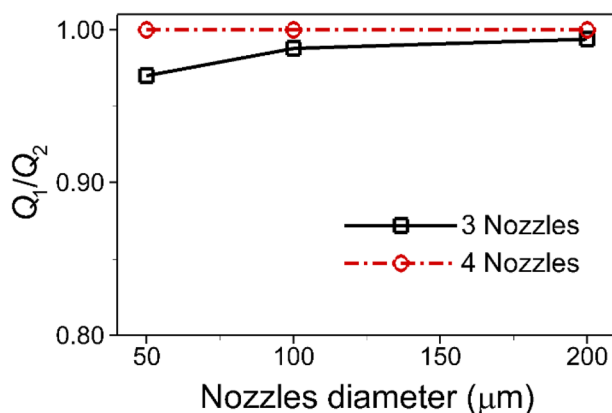

Fig. 4 Variation in the flow rate ratio at two nozzles, Q_1/Q_2, as a function of the nozzle diameter for three- and four-nozzle jets

to protect a jetting hole during nozzle wiping for maintenance, as shown in Fig. 5d, which presents a three dimensional schematic diagram of a single micro nozzle structure. Figure 5e is a SEM image of the magnified nozzle structure. The micro multi-nozzle jet plate was completed by affixing the multi-nozzle jet head to an ink reservoir block by adhesive bonding (Fig. 5f).

To make a thin film on the large area substrate by the nozzle coating process, the ink was coated by repetitively moving the head with the fixed head overlapping interval along the coating trajectory as shown in Fig. 1a. Prior to the coating process, it is very important to make a stable column jet flow because we can control the coating thickness by regulating the flow rate by control of the applied jetting pressure in the state of making the column jet flow. In this study, we proposed a unique nozzle jetting method that applies vacuum suction to the side of the jetting nozzle for the formation of a stable column jet flow. The micro multi-nozzle

jet head was designed and fabricated to operate in both the jetting and suction modes selectively or simultaneously, as shown in Fig. 5. Generally, in the first stage, the nozzle jet forms a dangling droplet at the nozzle end, and then the jetting pressure is further increased, and the dangling droplet drops and a continuous flow occurs, as shown in Fig. 6a. In our experiment without vacuum suction control, for the single nozzle, we increased the applied jetting pressure up to 30 kPa to create a continuous column jet flow, and then the jetting pressure was lowered to the target jetting pressure of 10 kPa for 15 s to stabilize the flow rate for the coating process. However, when the suction pressure of 90 kPa was applied to the side of the jetting nozzle through the side suction channel, as shown in Fig. 6b, a stable column jet flow was instantly formed by the applied target pressure of 10 kPa within 1 s without any dangling droplet at the end of the nozzle.

To perform a feasibility test of the developed micro multi-nozzle jet head for the large area and uniform thin film coating application, we selected EtOH-diluted PEDOT:PSS solution as a test ink. In our previous study, we investigated the ink formulation of PEDOT:PSS used as a hole injection layer (HIL) in an OLED structure for single nozzle coating. PEDOT:PSS is widely used in various organic optoelectronic devices. As a result, the optimized thickness uniformity was obtained at 90% EtOH volume concentration in PEDOT:PSS solution. In single nozzle coating using a SUSS needle of internal diameter = 100 μm, we could obtain a 4 mm wide and 20 nm thick PEDOT:PSS film suitable for OLED device fabrication with a printing speed of 1 m/s and an ink injection rate of 2 ml/min. From the previous results, we selected a PEDOT:PSS solution diluted by EtOH with a 90 vol% as a test ink [28]. The viscosity and surface tension values of the PEDOT: PSS solution were 10.5 cP and 71 mN/m before dilution. After dilution with 90% volume
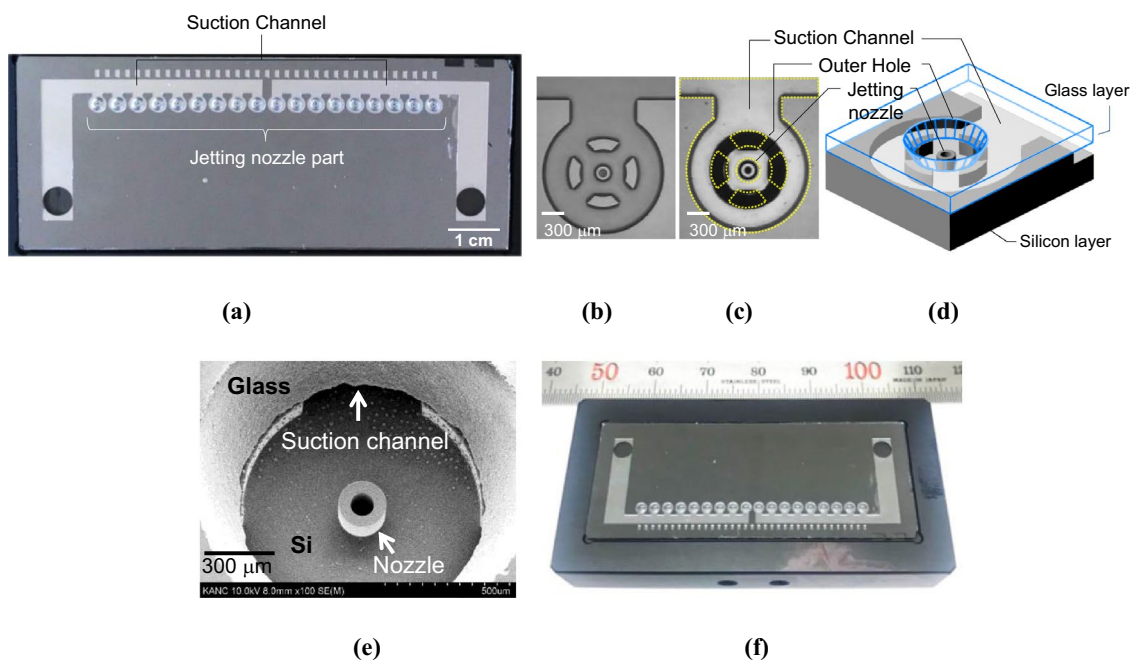
Fig. 5 Micro fabrication results: **a** microscopic image of the micro multi-nozzle jet head, **b** microscopic image of Si microstructure with a jetting nozzle and a suction channel, **c** microscopic image of the microstructure of the completed micro nozzle jet head by bonding the glass substrate, **d** three dimensional schematic diagram of a single micro nozzle structure, **e** SEM image of the magnified nozzle structure, **f** microscopic image of the micro multi-nozzle jet plate

ratio EtOH, its viscosity and surface tension were measured at 1.4 cP, and 23.8 mN/m, respectively.

Prior to large area and uniform thin film coating, we investigated the coating uniformity of the thin film by changing the applied jetting pressure and the printing pitch of the micro multi-nozzle jet head, as depicted in Fig. 1a. The ITO-coated glass substrate was treated by the atmospheric DC plasma surface treatment system for 30 s to obtain a hydrophilic surface before coating process. The initial contact angle of the EtOH-diluted PEDOT:PSS on the glass was about 24.8°, but its contact angle decreased to less than 5° after plasma surface treatment for 30 s. This means that the plasma surface treatment turns the glass surface into a hydrophilic (high energy) surface, allowing the EtOH diluted PEDOT:PSS to be perfectly wetted.

First, the width of the PEDOT:PSS film pattern was measured after single printing with the micro multi-nozzle jet head. EtOH diluted PEDOT:PSS solution was jetted under conditions of a head moving speed of 1 m/s, a coating gap distance between the nozzle and substrate of ~ 1 mm. The size of the ITO-coated glass substrate used in the experiment was 200×200 mm^2. Figure 7a shows cross sectional schematic illustration of the micro multi-nozzle jet head connected with the ink supply lines during coating process and Fig. 7b is a photograph of stable column jet flow formation. The width (W_{coated}) of the PEDOT:PSS film pattern was measured as ~ 47 mm, which is about 37% wider than the entire 18 nozzle width (W_{nozzle}) of 34.2 mm. The printed PEDOT:PSS pattern showed the coffee ring phenomenon at the edge areas, as shown in the microscopic image of Fig. 7c. The thickness line profile of the printed PEDOT:PSS pattern was measured at 1 mm intervals using the spectral reflectance system (Fig. 7d).

An average thickness and its uniformity of the 1 time printed PEDOT:PSS films were analyzed by changing the jetting pressure from 160 to 220 kPa at 20 kPa intervals. As seen in Fig. 8, the average thickness of the PEDOT:PSS films increased from 58.79 nm to 75.32 nm as the printing pressure increased. The best thickness uniformity was 4.8% at 180 kPa. The thickness of the PDDOT:PSS film coated at 180 kPa was 62.25 ± 2.99 nm. Thickness analysis was performed for a 40 mm wide pattern excluding a 3 mm wide coffee ring region at the edge of the printed pattern. The coffee ring region was excluded from the thickness analysis because the width of coffee ring region was negligible to less than 1% of 5th generation size (1100×1300 mm^2), the final target substrate size. The height of the pattern edge was about 100 nm due to the coffee ring phenomenon (Fig. 7d).

To apply a single printing method to scalable coating for large area organic thin film deposition, EtOH-diluted PEDOT:PSS solution was coated by the multi-nozzle jet coating method described in Fig. 1a by changing the printing pitch from 25 to 40 mm at 5 mm intervals. Here, the printing pitch is defined as the distance that the stage moved

Fig. 6 Schematic illustration, microscopic images at the end of nozzle, and pressure versus time chart for **a** general nozzle jet process and **b** suction mode nozzle jet process
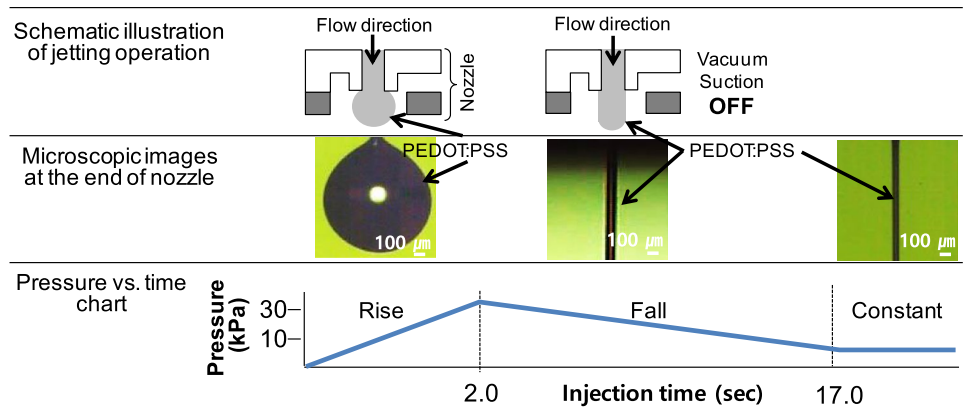

(a)
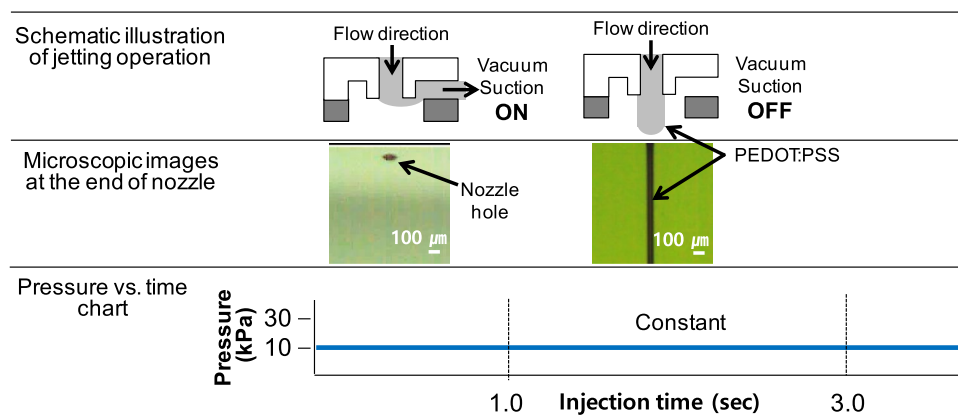
(b)

along the y-axis at a criterion of the head center point. The jetting pressure was 180 kPa which showed the best uniformity in the single printing experiment. As seen in Fig. 9, the average thickness of the PEDOT:PSS films decreased from 94.17 to 58.12 nm as the printing pitch increased. The coffee ring phenomenon was still observed on the edge region of the coated thin film. The thickness was measured for a 140 ~ 160 mm wide pattern excluding a 10 mm wide coffee ring region at the edge of the printed pattern. The width of the coffee ring regions was negligible to 1.53% level of 5th generation size (1100×1300 mm^2), the final target substrate size. From a line scan thickness analysis, the line profiles showed periodical waviness in the case of the thin films coated with a printing pitch of 25, 30 and 40 mm, but for a PEDOT: PSS film coated with a 35 mm print pitch, the line profile showed thickness uniformity (CV: coefficient of variation) of 3.87%. Finally, for the feasibility test of large area thin film coating, we coated a PEDOT:PSS thin film on a 5th generation size (1100×1300 mm^2) glass substrate by the developed micro multi-nozzle jet coating head with 35 mm printing pitch. Then, after splitting the 5th generation size

glass substrate into 40 pieces, the thickness and uniformity of each 40 samples were measured using a spectroscopic reflectometer. The measured thickness was 76.86 ± 3.33 nm and its uniformity (CV) was 4.33% excluding a 10 mm wide coffee ring region at the edge of the printed pattern. Figure 10a shows a cross sectional SEM image of the micro multi-nozzle jet coated PEDOT:PSS thin film of ~ 77 nm thickness.

The surface topography of PEDOT:PSS films deposited on the ITO-coated glass substrate was analyzed by AFM to compare the micro multi-nozzle jet coating method versus the conventional spin coating method, which is generally used in coating flat and uniform organic thin films. Figure 10b–d show AFM images of a 1×1 μm^2 scanned area on a bare ITO surface, a spin-coated PEDOT:PSS film surface, and a nozzle jet-coated PEDOT:PSS film surface, respectively. The center-line average roughness (R_a) and peak-to-valley roughness (R_{p-v}) of bare ITO are 13.47 and 143.23 nm. The R_a/R_{p-v} values of spin-coated and nozzle jet-coated PEDOT:PSS films are 1.01 nm/9.02 nm, and 1.07 nm/8.70 nm, respectively. R_a and R_{p-v} of the spin and
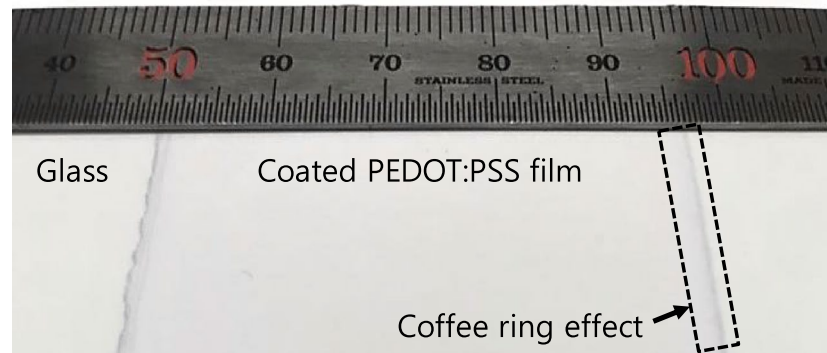
Fig. 7 **a** A cross sectional schematic illustration of the micro multi-nozzle jet head connected with the ink supply lines during coating process, **b** a photograph of stable column jet flow formation, **c** a photograph of the 1 time printed PEDOT:PSS pattern, and **d** a thickness profile of the 1 time printed PEDOT:PSS pattern
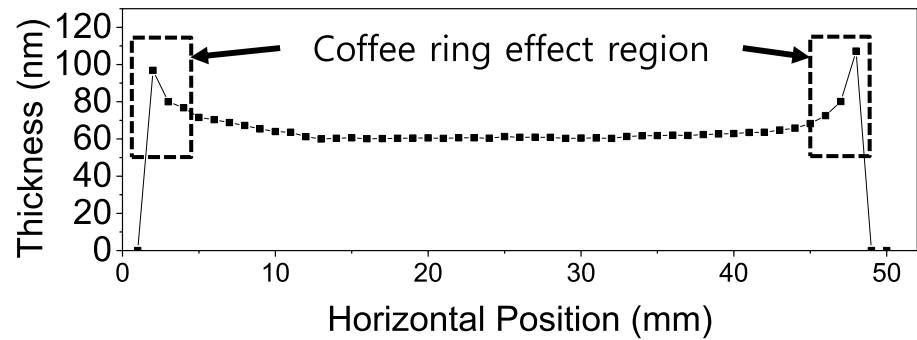

(a)

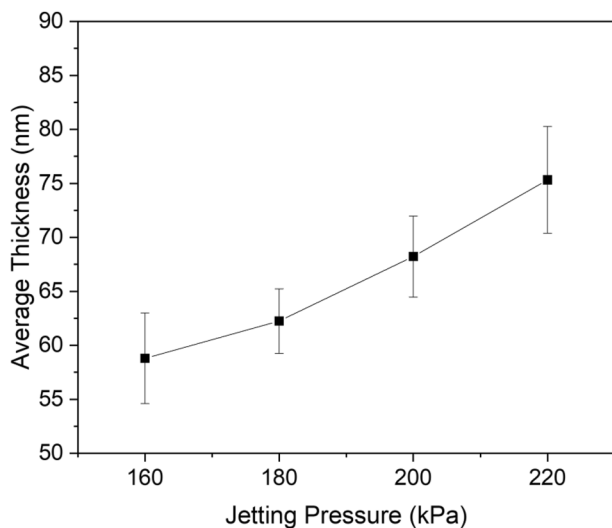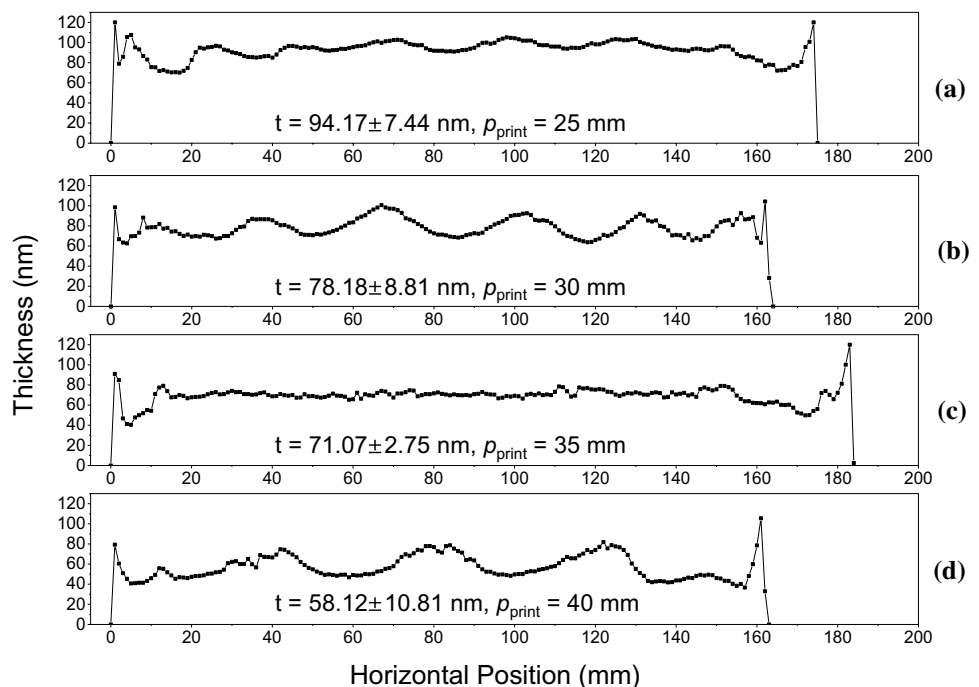Stable column jet flow
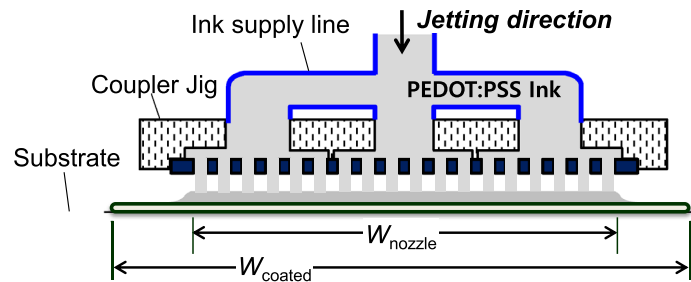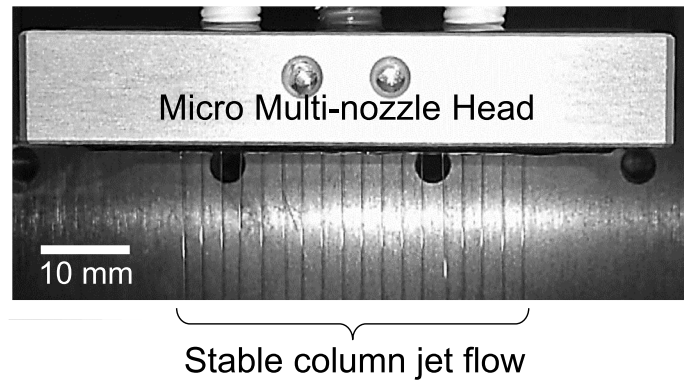
(b)

(c)

(d)

Fig. 8 Average thickness change of the 1 time printed PEDOT:PSS films according to the applied jetting pressure of 160, 180, 200, and 220 kPa
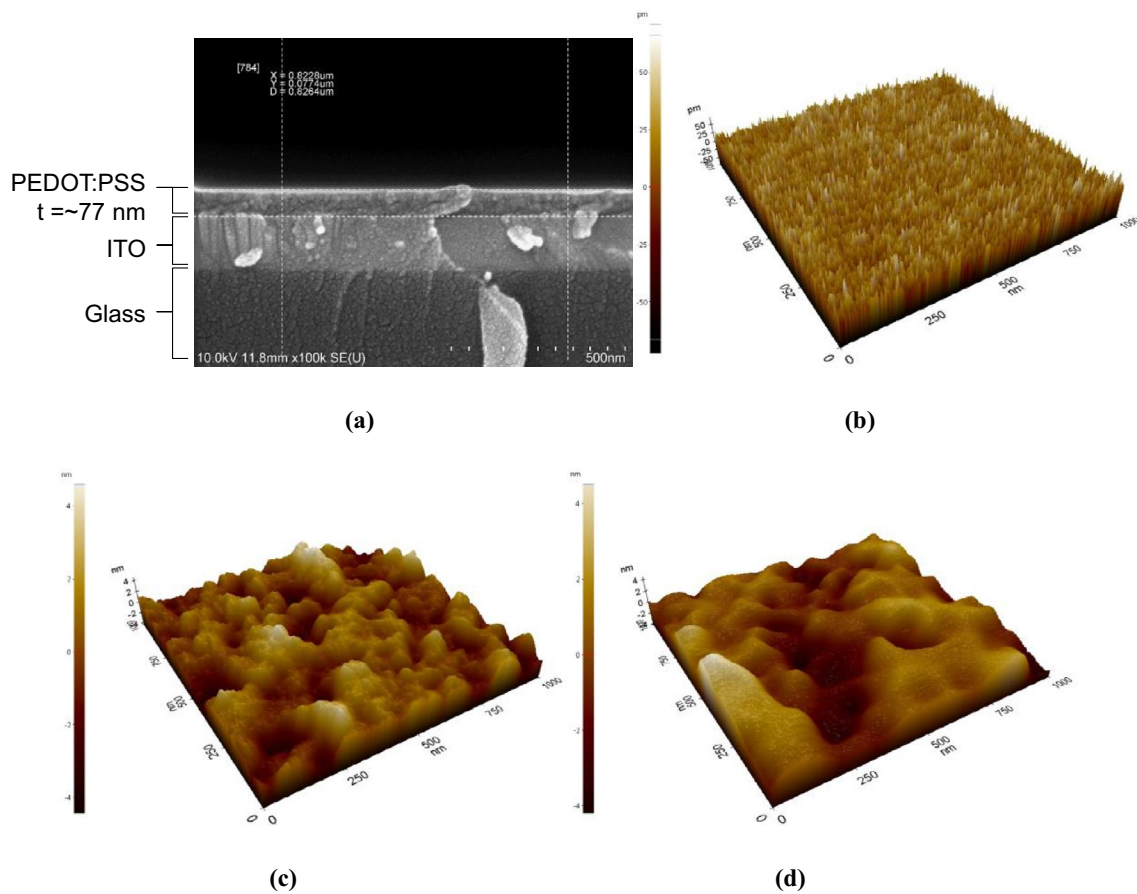
nozzle jet-coated PEDOT:PSS film surface was significantly lower than that of the bare ITO surface. The nozzle jet-coated PEDOT:PSS film surface showed larger grain surface compared to the spin-coated PEDOT:PSS film, but the nozzle jet-coated PEDOT:PSS films showed surface roughness very similar with spin-coated films.

4 Conclusions

This study developed a unique nozzle jetting method to form a stable column jet flow by removal of a dangling drop formation step that occurs in the general nozzle jet coating method. Vacuum suction to the side of the jetting nozzle is very effective for quick formation of a stable column jet flow. The micro multi-nozzle jet head was designed and fabricated to operate in both the jetting and suction modes. By a silicon micromachining process and an anodic bonding process, eighteen nozzles of 100 µm diameter were formed with 2 mm intervals and two suction channels were formed at both ends of the nozzle array. The stable column jet flow was instantly formed by control of the suction pressure and jetting pressure within 1 s. This study successfully demonstrated the micro multi-nozzle jet head based coating method applicable to a large area organic thin film coating. We coated a PEDOT:PSS thin film on a 5th generation size (1100×1300 mm^2) glass substrate by the developed micro multi-nozzle jet coating method. A uniform PEDOT:PSS thin film was obtained by conditioning physical parameters such as the jetting pressure, stage moving speed, and coating head printing pitch. The average thickness of the PEDOT:PSS thin film was 76.86 ± 3.33 nm and the uniformity (CV) was 4.33% under conditions of 1 m/s head moving speed and 180 kPa jetting pneumatic pressure excluding a coffee ring region. Also, the nozzle jet-coated PEDOT:PSS films showed surface roughness that was very similar with the spin-coated films from the AFM analysis.

Fig. 9 Line scan thickness analysis of the PEDOT:PSS films according to the printing pitch: **a** 25 mm, **b** 30 mm, **c** 35 mm, **d** 40 mm

(a)

(b)

(c)

(d)

Fig. 10 Cross sectional and surface analysis results of PEDOT:PSS thin film coated by micro multi-nozzle jet head: **a** cross sectional SEM image, **b** AFM image of bare ITO substrate surface before coating, **c** AFM image of spin-coated surface, **d** AFM image of nozzle jet-coated surface

Availability of Data and Materials The datasets supporting the conclusions of this article are included within the article.

Declarations

Conflict of interest There is no potential conflicts of interests/competing interests.

References

1. Cao, W., Li, J., Chen, H., & Xue, J. (2014). Transparent electrodes for organic optoelectronic devices: A review. *Journal of Photon Energy, 4,* 040990–040991. https://doi.org/10.1117/1.jpe.4.040990

2. Forrest, S. R. (2004). The path to ubiquitous and low-cost organic electronic appliances on plastic. *Nature, 428,* 911–918. https://doi.org/10.1038/nature02498

3. Espinos, N., Hosel, M., Angmo, D., & Krebs, F. C. (2012). Solar cells with one-day energy payback for the factories of the future. *Energy and Environmental Science, 5,* 5117–5132. https://doi.org/10.1039/c1ee02728j

4. Cao, W., & Xue, J. (2014). Recent progress in organic photovoltaics: Device architecture and optical design. *Energy and Environmental Science, 7,* 2123–2144. https://doi.org/10.1039/c4ee00260a

5. Choi, K.-J., Lee, J.-Y., Shin, D.-K., & Park, J. (2016). Investigation on slot-die coating of hybrid material structure for OLED lightings. *Journal of Physics and Chemistry of Solids, 95,* 119–128. https://doi.org/10.1016/j.jpcs.2016.04.006

6. Raupp, S. M., Merkleina, L., Pathak, M., Scharfer, P., & Schabela, W. (2017). An experimental study on the reproducibility of different multilayer OLED materials processed by slot die coating. *Chemical Engineering Science, 160,* 113–120. https://doi.org/10.1016/j.ces.2016.11.018

7. Choi, K.-J., Lee, J.-Y., Park, J., & Seo, Y.-S. (2015). Multilayer slot-die coating of large-area organic light-emitting diodes. *Organic Electronics, 26,* 66–74. https://doi.org/10.1016/j.orgel.2015.07.025

8. Gorter, H., Coenen, M. J. J., Slaats, M. W. L., Ren, M., Lu, W., Kuijpers, C. J., & Groen, W. A. (2013). Toward inkjet printing

of small molecule organic light emitting diodes. *Thin Solid Films, 532,* 11–15. https://doi.org/10.1016/j.tsf.2013.01.041

9. Wengeler, L., Schmitt, M., Peters, K., Scharfer, P., & Schabel, W. (2013). Comparison of large scale coating techniques for organic and hybrid films in polymer based solar cells. *Chemical Engineering and Processing: Process Intensification, 68,* 38–44. https://doi.org/10.1016/j.cep.2012.03.004

10. Krebs, F. C. (2009). All solution roll-to-roll processed polymer solar cells free from indium-tin-oxide and vacuum coating steps. *Organic Electronics, 10,* 761–768. https://doi.org/10.1016/j.orgel.2009.03.009

11. Søndergaard, R. R., Hosel, M., & Krebs, F. C. (2012). Roll-to-roll fabrication of large area functional organic materials. *Journal of Polymer Science Part B: Polymer Physics, 51,* 16–34. https://doi.org/10.1002/polb.23192l

12. Carvalho, M. S., & Kheshgi, H. S. (2000). Low-flow limit in slot coating: Theory and experiments. *Journal AIChE, 46,* 1907–1917. https://doi.org/10.1002/aic.690461003l

13. Koo, J., Kim, J. W., Kim, M., Yoon, S., & Shim, J. H. (2020). Inkjet printing of silica aerogel for fabrication of 2-D patterned thermal insulation layers. *International Journal of Precision Engineering and Manufacturing-Green Technology.* https://doi.org/10.1007/s40684-020-00189-4

14. Kang, M. G., & Kang, K.-T. (2018). Flexible 2-layer paper printed circuit board fabricated by inkjet printing for 3-D origami electronics. *International Journal of Precision Engineering and Manufacturing-Green Technology, 5*(3), 421–426. https://doi.org/10.1007/s40684-018-0045-2

15. Patil, S. A., Ryu, C.-H., & Kim, H.-S. (2018). Synthesis and characterization of copper nanoparticles (Cu-Nps) using rongalite as reducing agent and photonic sintering of Cu-Nps ink for printed electronics. *International Journal of Precision Engineering and Manufacturing-Green Technology, 5*(2), 239–245. https://doi.org/10.1007/s40684-018-0024-7

16. Jang, Y.-R., Ryu, C.-H., Hwang, Y.-T., & Kim, H.-S. (2020). Optimization of intense pulsed light sintering considering dimensions of printed Cu nano/micro-paste patterns for printed electronics. *International Journal of Precision Engineering and Manufacturing-Green Technology.* https://doi.org/10.1007/s40684-019-00180-8

17. Lee, J., Kim, S., & Lee, C. (2019). Surface drying for brittle material coating without crack defects in large-area roll-to-roll coating system. *International Journal of Precision Engineering and Manufacturing-Green Technology, 6*(4), 723–730. https://doi.org/10.1007/s40684-019-00104-6

18. Chesterfield, R., Johnson, A., Lang, C., Stainer, M., & Ziebarth, J. (2011). Solution-coating technology for AMOLED displays. *Information Display, 1*(11), 24–30. https://doi.org/10.1002/j.2637-496x.2011.tb00339.x

19. Bhamidipati, K. L., Didari, S., & Harris, T. A. L. (2013). Slot die coating of poly benzimiazole based membranes at the air engulfment limit. *Journal of Power Sources, 239,* 382–392. https://doi.org/10.1016/j.jpowsour.2013.03.132

20. Larsen-Olsen, T. T., Andreasen, B., Andersen, T. R., Bottiger, A. P. L., Bundgaard, E., Norrman, K., Andreasen, J. W., Jørgensen, M., & Krebs, F. C. (2012). Simultaneous multilayer formation of the polymer solar cell stack using roll-to-roll double slot-die coating from water. *Solar Energy Materials and Solar Cells, 97,* 22–27. https://doi.org/10.1016/j.solmat.2011.08.026

21. Chesterfield, R. J., Frischknecht, K. D., Stainer, M., & Truong, N. (2009). Multinozzle printing: A cost-effective process for OLED display fabrication. *Journal SID, 09,* 951–954. https://doi.org/10.1889/1.3256956

22. Kang, Y. J., Bail, R., Lee, C. W., & Chin, B. D. (2019). Inkjet printing of mixed-host emitting layer for electrophosphorescent organic light-emitting diodes. *Applied Materials & Interfaces, 11,* 21784–21794. https://doi.org/10.1021/acsami.9b04675

23. Kim, H., Lee, S., Han, D., & Yoo, S. (2014). High-density organic photovoltaic modules: Mask-free fabrication using nozzle jet printing and oblique deposition. *Solar Energy Materials and Solar Cells, 120,* 561–565. https://doi.org/10.1016/j.solmat.2013.09.039

24. Bhat, K. S., Ahmad, R., Yoo, J.-Y., & Hahn, Y.-B. (2018). Fully nozzle-jet printed non-enzymatic electrode for bio sensing applicaiton. *Journal of Colloid and Interface Science, 512*(2018), 480–488. https://doi.org/10.1016/j.jcis.2017.10.088

25. An, K., Yoon, D. G., & Kang, K.-T. (2020). Effects of residual solvent in printed phosphorescent emissive thin films as, the origin of limited efficiency in organic light emitting diodes. *Progress in Organic Coatings, 147,* 105781. https://doi.org/10.1016/j.porgcoat.2020.105781

26. An, K., Kim, J. B., Yoon, D. G., Jeong, Y.-C., & Kang, K.-T. (2019). P-72: Nozzle jet printing of organic thin films for solution process of organic light emitting diodes. *SID Symposium Digest of Technical Papers, 1,* 1503–1506. https://doi.org/10.1002/sdtp.13227

27. An, K., Kim, J. B., Yoon, D. G., Jeong, Y.-C., & Kang, K.-T. (2019). High speed nozzle jet printing for bendable organic light emitting diodes. *Flexible and Printed Electronics, 4*(1), 015009. https://doi.org/10.1088/2058-8585/AB0B9E

28. Yoon, D. G., Kang, M. G., Kim, J. B., & Kang, K.-T. (2018). Nozzle printed-PEDOT:PSS for organic light emitting diodes with various dilution rates of ethanol. *Applied Sciences, 8,* 203. https://doi.org/10.3390/app802020

Publisher's Note Springer Nature remains neutral with regard to jurisdictional claims in published maps and institutional affiliations.

Kwon-Yong Shin received bachelor of engineering in Aerospace Engineering from Chonbuk University in 2001 and Master of Engineering in Mechanical Design and Mechatronics from Hanyang University in 2010. He joined Korea Institute of Industrial Technology in 2004. His current research interests are in printed electronics and application of industrial inkjet technology.

Mingyu Kang received a Ph.D. degree from Seoul National University in 2020. He is currently a senior researcher in Package Development at SK Hynix. His research interests include advanced package and biocompatible packaging.

Myong-Ki Kim received bachelor of engineering in Mechatronics Engineering from Koreatech University in 2005 and Master of Engineering in Mechanical Engineering from Korea University in 2007. He joined Korea Institute of Industrial Technology in 2005~2013. Currently, he is working on semiconductors business at Deviceeng.

Ki Sung Jung is a graduate student in the Ph.D. program in the department of mechanical engineering at Ulsan National Institute of Science and Technology, Ulsan, South Korea. He received the M.E. degree in mechanical engineering from Ulsan National Institute of Science and Technology in 2018. His current research interests include computational fluid dynamics, combustion, and reducing pollutant emissions.

Chun Sang Yoo received the B.S. and M.S. degrees from Seoul National University in 1996 and 1998, respectively, and the Ph.D. degree from the University of Michigan in 2005, all in Mechanical Engineering. He is currently a Professor of Mechanical Engineering Department at Ulsan National Institute of Science and Technology (UNIST), and is serving as the Director of the UNIST Supercomputing Center. Prior to joining UNIST in 2009, he was a postdoctoral research fellow of Combustion Research Facility at Sandia National Laboratories (2006–2009) and a lecturer at the Republic of Korea Naval Academy (1998–2001). His research has focused on developing numerical methods for high-fidelity numerical simulations and investigating the characteristics of laminar/turbulent reacting/nonreacting flows using direct numerical simulations (DNS), large eddy simulations (LES), and Reynolds averaged Navier-Stokes simulations (RANS).

Kyung-Tae Kang received B.S. and Ph.D in Mechanical Engineering from Seoul National University in 1988 and 1994. Since joining the Korea Institute of Industrial Technology in 1996, he has worked on the research of the printed electronics applications and standardization using non-contact printing technologies such as an inkjet. His work also included fuel cell systems, solar cell, flexible circuit board and OLED display/light.

Sang-Ho Lee in 1996 and 1998, received B.S. and M.S., respectively from the Department of Metal Materials Engineering at Hanyang University. In 2003, he received Ph.D. from the School of Electrical Engineering and Computer Science at Seoul National University, and joined the Korea Institute of Industrial Technology in 2006 after completing two year post-doctoral fellowship at Soh Lab, UCSB. His current research interests are in microdevice-based bioanalysis, hybrid printed electronics and industrial application of the inkjet technology.